*Inorg. Chem.* **2004**, *43*, 1472–1480

# A Geometrically Constraining Bis(benzimidazole) Ligand and Its Nearly Tetrahedral Complexes with Fe(II) and Mn(II)

**Robert T. Stibrany, Maxim V. Lobanov, Harvey J. Schugar,* and Joseph A. Potenza***

*Department of Chemistry and Chemical Biology, Rutgers, The State University of New Jersey, 610 Taylor Road, Piscataway, New Jersey 08854*

Received June 3, 2003

2,2′-Bis[2-(1-propylbenzimidazol-2-yl)]biphenyl), **4**, and its bis complexes with Fe(II) and Mn(II) have been prepared and characterized structurally and spectroscopically. Ligand **4** adopts an open, "trans" conformation in the solid state with the benzimidazole (BzIm) groups on opposite sides of the biphenyl unit. In its complexes with metal ions, a "cis" conformation is observed, and **4** behaves as a geometrically constraining bidentate ligand with four planar groups connected by three "hinges". Reaction of **4** with Fe(II) or Mn(II) yielded isomorphous crystals (space group *Pnn*2) of $Fe^{II}(\mathbf{4})_2\cdot(ClO_4)_2$ and $Mn^{II}(\mathbf{4})_2\cdot(ClO_4)_2$, in which the $M^{II}(\mathbf{4})_2$ cations exhibit distorted-tetrahedral coordination geometries (N–M–N angles, 109 ± 11°) enforced by rigid, chiral nine-membered M(**4**) rings in the twist–boat–boat conformation. Individually, the cations show *R*,*R* or *S*,*S* stereochemistry, and the crystals are racemates. $Mn^{II}(\mathbf{4})_2\cdot(ClO_4)_2$ exhibits a quasi-reversible Mn(II) → Mn(III) oxidation at $E_{1/2} = 0.64$ V; the corresponding Fe(II) → Fe(III) oxidation occurs at $E_{1/2} = 1.76$ V. The electrochemical stability of the Fe(III) oxidation state in this system suggests the possibility of isolating an unusual pseudotetrahedral $Fe^{III}N(BzIm)_4$ species. Ultraviolet spectra of the iron and manganese complexes are dominated by absorptions of the ligand **4** blue-shifted by approximately 2000–3000 $cm^{-1}$. Ligand-field absorptions were observed for the Fe(II) complex; those for the Mn(II) complex were obscured by tailing ultraviolet absorptions. Electron paramagnetic resonance and magnetic susceptibility measurements are consistent with a high-spin Mn(II) complex, while for the Fe(II) complex, the falloff of the magnetic moment with decreasing temperature is indicative of zero-field splitting with $D \sim 4$ $cm^{-1}$.

## Introduction

Multidentate ligands designed to constrain the coordination geometries of metals have found several applications in chemistry. For example, geometrically constraining ligands have been used as polymerization catalysts,[1] which have spawned a large academic and industrial research effort,[2] one which continues today.[3] These group IV catalysts have also been reported to be efficient hydrosilation catalysts.[4] Further, geometrically constraining ligands have been used to effect a particular coordination geometry, such as trigonal-pyramidal,[5] or an unusual oxidation state, such as Ni(I),[6] or to ensure the formation of a given isomer.[7] In bioinorganic chemistry, they have been used extensively to help model the active sites of metalloproteins.[8] Some time ago, we designed the bis(imidazole)biphenyl-based bidentate ligand **7** as a tetrahedrally constraining moiety to study the electronic features and Cu(I)/Cu(II) electron self exchange

* Authors to whom correspondence should be addressed. E-mail: schugar@rutchem.rutgers.edu (H.J.S.); potenza@rutchem.rutgers.edu (J.A.P.).

(1) (a) Shapiro, P. J.; Bunel, E.; Schaefer, W. P.; Bercaw, J. E. *Organometallics* **1990**, *9*, 867−869. (b) Canich, J. A. M. U.S. Patent 5,026,798, 1991.
(2) McKnight, A. L.; Waymouth, R. M. *Chem. Rev.* **1998**, *98*, 2587−2598.
(3) (a) Zi, G.; Li, H.-W.; Xie, Z. *Organometallics* **2002**, *21*, 3850−3855. (b) Wang, H.; Wang, Y.; Li, H.-W.; Xie, Z. *Organometallics* **2001**, *20*, 5110−5118. (c) Juvaste, H.; Pakkanen, T. T.; Iiskola, E. I. *J. Organomet. Chem.* **2000**, *606*, 169−175. (d) Lanza, G.; Fragalà, I. L.; Marks, T. J. *J. Am. Chem. Soc.* **2000**, *122*, 12764−12777. (e) Juvaste, H.; Pakkanen, T. T.; Iiskola, E. I. *Organometallics* **2000**, *19*, 1729−1733. (f) Lu, H. L.; Hong, S.; Chung, T. C. *Macromolecules* **1998**, *31*, 2028−2034.
(4) Trifonov, A. A.; Spaniol, T. P.; Okuda, J. *Organometallics* **2001**, *20*, 4869−4874.
(5) Raab, V.; Kipke, J.; Burghaus, O.; Sundermeyer, J. *Inorg. Chem.* **2001**, *40*, 6964−6971.
(6) Dietrich-Buchecker, C. O.; Guilhem, J.; Kern, J.-M.; Pascard, C.; Sauvage, J.-P. *Inorg. Chem.* **1994**, *33*, 3498−3502.
(7) Bond, A. M.; Colton, R.; Kevekordes, J. E.; Panagiotidou, P. *Inorg. Chem.* **1987**, *26*, 1430−1435.
(8) (a) Lee, W.-Z.; Tolman, W. B. *Inorg. Chem.* **2002**, *41*, 5656−5658. (b) Holland, P. L.; Tolman, W. B. *J. Am. Chem. Soc.* **2000**, *122*, 6331−6332. (c) Randall, D. W.; George, S. D.; Hedman, B.; Hodgson, K. O.; Fujisawa, K.; Solomon, E. I. *J. Am. Chem. Soc.* **2000**, *122*, 11620−11631 and references therein.



10.1021/ic030180o CCC: $27.50 
Published on Web 01/17/2004

for the structurally similar, distorted-tetrahedral tetrakis(imidazole)$Cu^{I}$(**7**)$_2$ and $Cu^{II}$(**7**)$_2$ coordination geometries.[9] Recently, we found that 2,2′-bis[2-(1-propylbenzimidazol-2-yl)]biphenyl (**4**), an alkylated benzimidazole analogue of **7**, forms more nearly tetrahedral complexes with divalent first-row transition metals ranging from Cr(II) to Zn(II) and also acts as a highly basic proton sponge.[10] In some instances, one bis(benzimidazole) species such as the ligand in **8**[11a] or ligand **4**[11b,c] is sufficient to constrain the coordination geometry substantially toward tetrahedral (e.g., with X = N or Cl, the following ranges were found: for $Mn^{II}$(**8**)$Cl_2$, X−Mn(II)−X′, 96.8−115.7°;[11a] $Ni^{II}$(**4**)$Cl_2$, X−Ni(II)−X′, 102.1−123.4°;[11b] $Cu^{II}$(**4**)$Cl_2$, X−Cu(II)−X′, 96.6−133.7°[11c]). We report here the preparation and characterization of **4** and its complexes with Fe(II) and Mn(II); corresponding complexes with Cr(II), Co(II), Ni(II) Cu(I,II), and Zn(II) will be described later.[12] We expect the $Cu^{I}$(**4**)$_2$/$Cu^{II}$(**4**)$_2$ pair to be particularly useful for the study of Cu(I)/Cu(II) electron self exchange.[9,13]

## Experimental Section

All reagents were used as received or purified by standard methods.[14] Melting points were determined with a hot-stage apparatus and are uncorrected. Densities of the crystalline products were measured by flotation.

**Safety Note.** We experienced no difficulty handling these materials, but it should be noted that perchlorate salts of metal complexes with organic ligands are potentially explosive. Only small amounts of materials should be prepared, and these should be handled with great care.

**1. Preparation of the Complexes.** The preparation of the ligand diprpBBIL, **4**, and its complexes with Fe(II) and Mn(II) is described below and outlined in Scheme 1. The preparation and characterization of the corresponding Zn(II) complex of **4**, which is used as a spectroscopic reference in the present paper, will be reported elsewhere.[12]

**2,2′-Bis[2-(1-hydrobenzimidazol-2-yl)]biphenyl, HBBIL (3).** To a 150 mL round-bottom flask were added 5.00 g (20.6 mmol) of biphenyl-2,2′-dicarboxylic acid (**1**), 4.46 g (41.3 mmol) of 1,2-phenylenediamine (**2**), and 15 g of polyphosphoric acid (PPA) sequentially to give a thick paste. The magnetically stirred mixture was heated at 180 °C for 3.5 h, cooled to 100 °C, and neutralized to pH 8 by the slow addition of a concentrated ammonium hydroxide solution. The resulting solid was collected by filtration, washed repeatedly with water, and dried to a constant weight in a vacuum oven at 55 °C for 24 h. $C_{26}H_{18}N_4$, fw = 386.45. Yield: 15.32 g, 96%. Mp: 295 °C. $^1$H NMR ($CD_3SO_2CD_3$) $\delta$: 7.73 (d, $J$ = 7.5 Hz, 2H), 7.50 (q, $J$ = 3.5 Hz, 4H), 7.34 (t, $J$ = 7.0 Hz, 2H), 7.22 (t, $J$ = 7.0 Hz, 2H), 7.16 (q, $J$ = 3.0 Hz, 4H), 6.97 (d, $J$ = 7.5 Hz, 2H). $^{13}$C NMR ($CD_3SO_2CD_3$) $\delta$: 153.2, 141.0, 138.7, 130.6, 130.4, 130.0, 128.9, 127.4, 122.1, 115.2. $R_f$ = 0.36 (ethyl acetate). FD MS: 387.3. IR (KBr pellet, cm$^{-1}$): 1709 m, 1621 m, 1431 s, 1369 w, 1274 m, 744 s, 531 w, 429 w. Anal. Calcd for $C_{26}H_{18}N_4$: N, 14.50; H, 4.69; C, 80.81. Found: N, 14.41; H, 4.79; C, 80.65.

**Scheme 1**

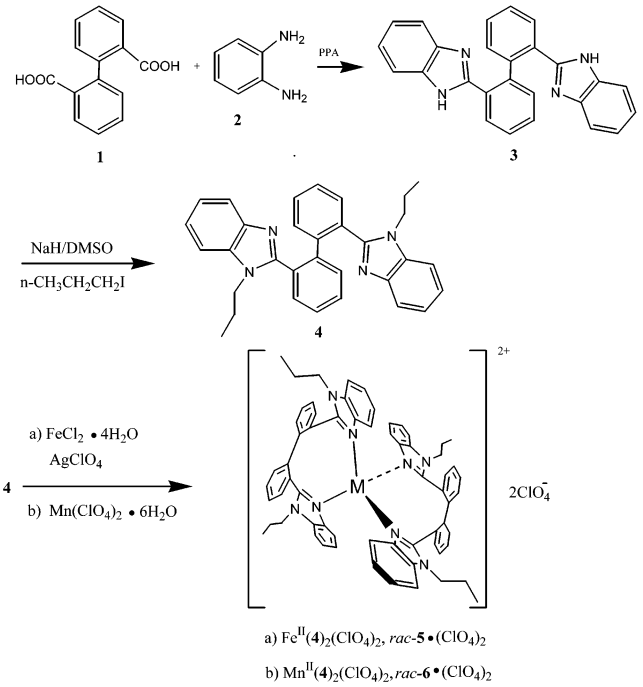


**2,2′-Bis[2-(1-propylbenzimidazol-2-yl)]biphenyl, diprpBBIL (4).** To a stirred mixture of 4.65 g (12.0 mmol) of **3** and 40 mL of dry DMSO in a 150 mL round-bottom flask fitted with a side arm and maintained under a nitrogen atmosphere was added 0.86 g of sodium hydride (95%) over 1 h, followed by the dropwise addition of 2.35 mL (24.1 mmol) of *n*-iodopropane over 1 h. The reaction mixture was stirred overnight, quenched with water, and then added to 400 mL of water. After stirring for $^1/_2$ h, a pale-pink precipitate was collected by filtration, washed repeatedly with water, and dried in a vacuum oven for 24 h at 60 °C. The crude product was dissolved in 100 mL of ethyl alcohol containing 5 g of activated charcoal, refluxed for 15 min, filtered hot, and recovered. Rotary evaporation of the solvent, followed by drying under high vacuum, gave a pale-orange amorphous solid. Yield: 5.32 g, 92%. Mp: 149 °C. Crystals suitable for X-ray diffraction were obtained by the slow evaporation of a solution of **4** in a mixture of ethyl alcohol and triethyl orthoformate. $^1$H NMR ($CD_3SO_2CD_3$) $\delta$: 7.51 (m, 6H), 7.36 (t, $J$ = 7.5 Hz, 2H), 7.20 (m, 6H), 7.02 (d, $J$ = 7.7 Hz, 2H), 3.42 (brd m, 4H), 1.65 (br m, 4H), 0.83 (t, $J$ = 7.3 Hz, 6H). $^{13}$C NMR ($CDCl_3$) $\delta$: 152.7, 143.1, 140.8, 134.8, 131.2, 131.0, 129.5, 127.2, 122.3, 121.8, 119.8, 110.1, 45.8, 22.9, 11.3. $R_f$ = 0.66 (ethyl acetate/silica). IR (KBr pellet, cm$^{-1}$): 3062 m, 2968 m, 2931 m, 2871 m, 1643 s, 1447 s, 1329 s, 1276 s, 1128 m, 743 s, 476 w. Anal. Calcd for **4**: N, 11.91; H, 6.42; C, 81.67. Found: N, 11.97; H, 6.21; C, 80.83.

***rac*-Bis{2,2′-bis[2-(1-propylbenzimidazol-2-yl)]biphenyl}iron(II) Bis(perchlorate), $Fe^{II}$(**4**)$_2$·(ClO$_4$)$_2$, *rac*-5·(ClO$_4$)$_2$.** Two equiv of **4** (520 mg, 1.10 mmol) was added to a stirred mixture of 110 mg (0.55 mmol) of $FeCl_2$·$4H_2O$, 20 mL of acetonitrile, and 5 mL of triethyl orthoformate. After 10 min, 229 mg (1.10 mmol) of $AgClO_4$ was added, and the mixture was stirred overnight and then filtered through a 0.2 $\mu$m poly(tetrafluoroethylene) membrane to

(9) Knapp, S.; Keenan, T. P.; Zhang, X.; Fikar, R.; Potenza, J. A.; Schugar, H. J. *J. Am. Chem. Soc.* **1990**, *112*, 3452−3464.
(10) Stibrany, R. T.; Schugar, H. J.; Potenza, J. A. *Acta Crystallogr.* **2002**, *E58*, o1142−o1144.
(11) (a) Broughton, V.; Bernardinelli, G.; Williams, A. F. *Inorg. Chim. Acta* **1998**, *275*, 279−288. (b) Stibrany, R. T.; Matturro, M. G.; Zushma, S.; Patil, A. O. U.S. Patent 6,501,000, 2002. (c) Stibrany, R. T.; Zushma, S.; Patil, A. O. 223rd ACS National Meeting, Orlando, FL, Apr 7−11, 2002; PMSE-56.
(12) Stibrany, R. T.; Schugar, H. J.; Potenza, J. A. To be published.
(13) (a) Ambundo, E. A.; Ochrymowycz, L. A.; Rorabacher, D. B. *Inorg. Chem.* **2001**, *40*, 5133−5138. (b) Xie, B.; Wilson, L. J.; Stanbury, D. M. *Inorg. Chem.* **2001**, *40*, 3606−3614. (c) Xie, B.; Elder, T.; Wilson, L. J.; Stanbury, D. M. *Inorg. Chem.* **1999**, *38*, 12−19.
(14) Perrin, D. D.; Armarego, W. L. F. *Purification of Laboratory Chemicals*; Pergamon Press: New York, 1988.

**Table 1.** Crystallographic Data for the Several Species Studied

| | diprpBBIL, **4** | $Fe^{II}(\mathbf{4})_2\cdot(ClO_4)_2$, *rac*-**5**·$(ClO_4)_2$ | $Mn^{II}(\mathbf{4})_2\cdot(ClO_4)_2$, *rac*-**6**·$(ClO_4)_2$ |
|---|---|---|---|
| formula | $N_4C_{32}H_{30}$ | $FeCl_2O_8N_8C_{64}H_{60}$ | $MnCl_2O_8N_8C_{64}H_{60}$ |
| fw | 470.61 | 1195.96 | 1195.05 |
| $a$ (Å) | 8.2663(17) | 15.290(4) | 15.2527(15) |
| $b$ (Å) | 16.200(3) | 17.226(4) | 17.1915(17) |
| $c$ (Å) | 39.351(8) | 11.119(3) | 11.0902(11) |
| $\beta$ (deg) | 90.700(3) | 90 | 90 |
| $V$ (Å$^3$) | 5269.2(18) | 2928.7(12) | 2908.0(5) |
| space group | $P2_1/n$ | *Pnn*2 | *Pnn*2 |
| $Z$ | 8 | 2 | 2 |
| $\rho_{calcd}$ (g/cm$^3$) | 1.186 | 1.356 | 1.365 |
| $\rho_{obsd}$ (g/cm$^3$) | 1.21(1) | 1.33(1) | 1.34(1) |
| $\mu$ (mm$^{-1}$) | 0.071 | 0.412 | 0.383 |
| trans factor | 0.79−1.00 | 0. 81−1.00 | 0.78−1.00 |
| $T$ (K) | 298(1) | 298(1) | 298(1) |
| data/parameters used in refinement | 8525/653 | 4449/383 | 5020/388 |
| $R_f$,[a] $Rw_f^2$ [b] | 0.069, 0.186 | 0.058, 0.164 | 0.064, 0.177 |

[a] $R_f = \sum||F_o| - |F_c||/\sum|F_o|$; selection criterion $I > 2\sigma(I)$. [b] $Rw_f^2 = \{[\sum[w(F_o^2 - F_c^2)^2/\sum[w(F_o^2)^2]\}^{1/2}$; selection criterion all of the $F_o^2$.

give a clear pale orange-brown solution. Vapor diffusion of diethyl ether into this filtrate afforded pale-orange-brown crystals suitable for X-ray diffraction, which were collected by filtration and dried in air. Yield: 606 mg, 92.1%. IR (KBr pellet, cm$^{-1}$): 3063 m, 2967 m, 2930 m, 1615 m, 1466 s, 1420 s, 1287 m, 1092 s, 907 s, 758 s, 621 m. Anal. Calcd for *rac*-**5**·$(ClO_4)_2$: N, 9.37; H, 5.06; C, 64.27; Cl, 5.93. Found: N, 9.64; H, 5.36; C, 64.09; Cl, 5.78.

***rac*-Bis{2,2′-bis[2-(1-propylbenzimidazol-2-yl)]biphenyl}-manganese(II) Bis(perchlorate), $Mn^{II}(\mathbf{4})_2\cdot(ClO_4)_2$, *rac*-6·2$(ClO_4)_2$.** In a similar fashion, a mixture containing 2 equiv of **4** (400 mg, 0.85 mmol), 154 mg (0.425 mmol) of $Mn(ClO_4)_2\cdot 6H_2O$, 20 mL of acetonitrile, and 2 mL of triethyl orthoformate was heated to reflux. Following vapor diffusion of diethyl ether into the room-temperature mixture, pale-yellow-brown crystals suitable for X-ray diffraction were deposited, collected by filtration, and dried in air. Yield: 480 mg, 94.5%. IR (KBr pellet, cm$^{-1}$): 3061 m, 2967 m, 2930 m, 1615 m, 1464 s, 1420 s, 1287 m, 1088 s, 903 s, 760 s, 623 m. Anal. Calcd for *rac*-**6**·2$(ClO_4)_2$: N, 9.38; H, 5.06; C, 64.32; Cl, 5.93. Found: N, 9.45; H, 5.29; C, 63.19; Cl, 6.09.

**2. Spectroscopic and Electrochemical Studies.** NMR spectra were recorded using a Bruker AVANCE 400 Ultrashield spectrometer. Infrared spectra were measured using a Mattson Galaxy series 5000 spectrophotometer. Electronic-spectral measurements were made using Cary instruments upgraded and computer-interfaced by Aviv Associates. Reflectance measurements were made using a Perkin-Elmer 330 spectrophotometer fitted with a 60 mm diameter integrating sphere. Electron paramagnetic resonance (EPR) spectra were measured with a Varian E-12 spectrometer calibrated with a Hewlett-Packard model 5245-L frequency counter and a diphenyl picrylhydrazyl crystal ($g = 2.0036$). Magnetic susceptibilities were measured from 2 to 295 K using a Quantum Design SQUID magnetometer (MPMS-XL) operated at 1000 Oe. Diamagnetic corrections for the sample holder and for the ligands and counterions (calculated from Pascal's constants) were applied to the susceptibilities.

All electrochemical measurements were carried out with a conventional three-electrode system. A glassy carbon disk of approximately 0.28 cm$^2$ surface area served as the working electrode. The reference electrode was a commercial saturated calomel electrode, and a platinum wire was used as the counter electrode.

Both differential pulse polarography (DPP) and cyclic voltammetry experiments were performed using a BAS 100B electrochemical analyzer interfaced to a PC. Potentials for the manganese oxidations were determined by DPP, while iron oxidation and reduction potentials were determined from cyclic voltammograms. All measurements were performed under nitrogen. Cyclic voltammetry measurements were made at scan rates of 25−300 mV/s. Differential pulse measurements were made at 4 mV/s. Calibration was checked against ferrocene. Solutions were made from HPLC-grade dichloromethane that was distilled from $CaH_2$. A stock solution (0.05 M) in tetra-*n*-butylammonium hexafluorophosphate was prepared. Solutions of the complexes were prepared having concentrations of $(1-2) \times 10^{-4}$ M.

**3. X-ray Crystallography.** Diffraction measurements were made with a Bruker SMART CCD area detector system using $\phi$ and $\omega$ scans. In all cases, a hemisphere of data was collected. Cell parameters were determined using the SMART software.[15a] The SAINT package[15a] was used for integration of data, and Lorentz, polarization, and decay corrections and for merging of data. Absorption corrections were applied using SADABS.[15b]

Structures were solved[15c] and refined[15d] on $F^2$ using the SHELX system and all of the data. Partial structures were obtained by direct methods; the remaining non-hydrogen atoms in each structure were located using difference Fourier techniques. H atoms were located on difference Fourier maps or placed at calculated positions. For H atoms whose thermal parameters were not refined, isotropic temperature factors were set equal to $1.2-1.5U_N$, where N is the atom bonded to H. Views of the structures were prepared using ORTEP32 for Windows.[16] Additional details of the data collection and refinement for the three crystals studied are given in Table 1 and in the Supporting Information.

## Results and Discussion

**1. Syntheses.** The preparation of benzimidazoles dates from the middle of the 19th century,[17] and condensation of 1,2-phenylenediamine with a host of organic functionalities to yield benzimidazoles has been well documented.[18] De-

(15) (a) Bruker. *SHELXTL*, version 6.10; Bruker AXS Inc.: Madison, WI, 2000. Bruker. *Saint-Plus*, version 6.02; Bruker AXS Inc.: Madison, WI, 2000. Bruker. *SMART-WNT2000*, version 5.622; Bruker AXS Inc.: Madison, WI, 2000. (b) Blessing, R. H. *Acta Crystallogr.* **1995**, *A51*, 33−38. (c) Sheldrick, G. M. SHELXS-97. *Acta Crystallogr.* **1990**, *A46*, 467−473. (d) Sheldrick, G. M. *SHELXL-97. A Computer Program for the Refinement of Crystal Structures*; University of Göttingen: Göttingen, Germany, 1997.
(16) Farrugia, L. J. *J. Appl. Crystallogr.* **1997**, *30*, 565.
(17) Heintz, W. *Anal. Chem.* **1862**, *123*, 325−341.

**Table 2.** Metric Parameters for the Species Studied (Å, deg)

| | $Fe^{II}(\mathbf{4})_2\cdot(ClO_4)_2$, *rac*-**5**·$(ClO_4)_2$ | $Mn^{II}(\mathbf{4})_2\cdot(ClO_4)_2$, *rac*-**6**·$(ClO_4)_2$ | diprpBBIL, **4** |
|---|---|---|---|
| M−N13 | 2.078(4) | 2.138(4) | |
| M−N43 | 2.078(4) | 2.130(4) | |
| intraligand | | | |
| N13−M−N43′ | 120.89(14) | 119.95(15) | |
| interligand | | | |
| N13−M−N13′ | 99.8(2)[a] | 100.8(2) | |
| N13−M−N43 | 108.35(15) | 107.60(15) | |
| N43−M−N43′ | 100.0(2) | 102.1(2) | |
| N11−C12[b] (amine) | 1.334(6), 1.335(6) | 1.350(7), 1.338(6) | 1.372(4), 1.374(4), 1.368(4), 1.380(4) |
| N13−C12[b] (imine) | 1.351(6), 1.330(6) | 1.339(7), 1.336(6) | 1.306(4), 1.311(3), 1.314(4), 1.311(4) |
| N11−C11[b] | 1.369(6), 1.397(7) | 1.373(6), 1.402(7) | 1.381(4), 1.381(4), 1.380(4), 1.387(4) |
| N13−C13[b] | 1.395(6), 1.395(6) | 1.391(7), 1.406(6) | 1.391(4), 1.389(4) 1.386(4), 1.382(4) |
| C11−C13[b] | 1.415(7), 1.366(7) | 1.402(7), 1.377(7) | 1.387(4), 1.391(4), 1.395(4), 1.389(4) |
| $\phi-\phi$[c] | 52.2(2) | 50.2(2) | 126.7(1), 129.9(1) |
| $\phi$-Bz1[d] | 56.9(1) | 56.7(2) | 52.2(1) |
| $\phi$-Bz2 | 59.3(1) | 58.0(1) | 62.1(1) |
| $\phi$-Bz3 | | | 64.51(8) |
| $\phi$-Bz4 | | | 67.33(9) |

[a] Symmetry transformation for *rac*-**5**·$(ClO_4)_2$: $2-x, -y, z$. That for *rac*-**6**·$(ClO_4)_2$: $-x, -y, z$. [b] Successive entries for a given crystal are for imidazole fragments containing N11, N41, N51, and N81, respectively. [c] $\phi-\phi$ is the dihedral angle between the phenyl rings. [d] Bz1 through Bz4 stand for benzimidazole rings containing N11, N41, N51, and N81, respectively.

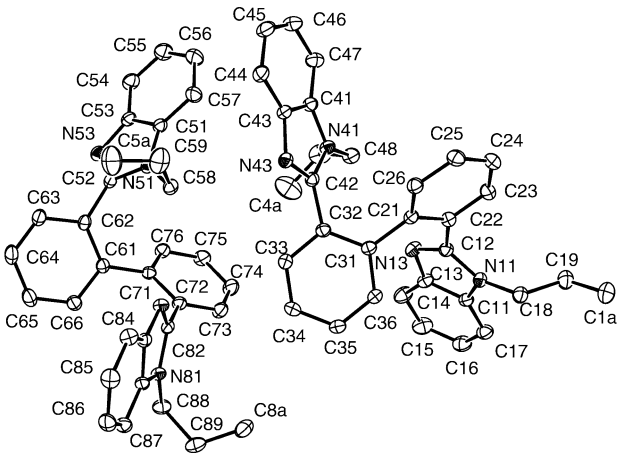


**Figure 1.** View of the two unique molecules of **4**. H atoms have been omitted for clarity.

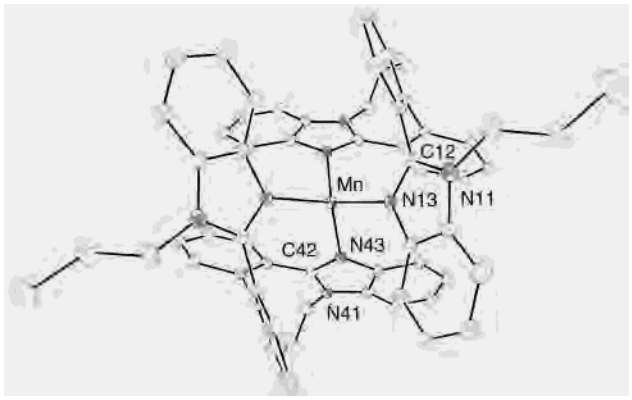


**Figure 2.** View along the 2-fold axis (001 direction) of one of the enantiomeric cations in *rac*-**6**. H atoms have been omitted for clarity.

hydration is an important factor in the condensation of carboxylic acids with 1,2-phenylenediamine. We have found that our modified use of polyphosphoric acid, a reagent often used in the past for benzimidalole syntheses,[19] as a reaction medium affords a superior acid catalyst/dehydration medium for achieving high-yielding, rapid production of the target benzimidazoles reported in the present paper. Further, while numerous methods for the alkylation of benzimidazoles have been reported,[18] we have found that the modification of a known alkylation procedure[20] reported here gives excellent results for this class of biphenylbenzimidazoles.

**2. Description of the Structures.** Ligand **4** crystallizes in space group $P2_1/n$ with two molecules in the asymmetric unit (Figure 1). Its bis complexes with Fe(II), *rac*-**5**·$(ClO_4)_2$, and Mn(II), *rac*-**6**·$(ClO_4)_2$, crystallize in space group *Pnn*2 and are isomorphous. A view of one of the cations in *rac*-**5**, which is isostructural with *rac*-**6**, is shown in Figure 2. In each structure, the benzimidazole and phenyl groups are planar to within 0.01−0.02 Å, and ligand flexibility is provided by the torsional twist about the C−C bonds linking the planar groups. In effect, **4** behaves as a three-hinged species. As suggested by the phenyl−phenyl dihedral angles (Table 2), the free and bound ligands **4** exhibit significantly different conformations; **4** adopts an extended, "trans" conformation with the benzimidazole fragments on opposite sides of the biphenyl group, while the bound ligands are of necessity the "cis" conformation. In **4**, the C12−N13 distances (Table 2) are significantly shorter than the C12−N11 distances, implying substantial imine and amine character, respectively, for these linkages. Ligation results in effectively equal C12−N13 and C12−N11 distances in *rac*-**5** and *rac*-**6**, consistent with the electron delocalization over the N11−C12−N13 units, a common feature of imidazolium and benzimidazolium salts.[10] In the crystal, molecules of **4** pack with little or no $\pi$ overlap among the several aromatic groups. In contrast, the ethyl analogue of **4** adopts an unusual, compact, twisted-clamshell conformation with intramolecular

(18) Grimmett, M. R. In *Imidazole and Benzimidazole Synthesis*; Meth-Cohn, O., Ed.; Academic Press: San Diego, CA, 1997.
(19) (a) Vyas, P. C.; Oza, C. K.; Goyal, A. K. *Chem. Ind.* **1980**, 287−288. (b) Hein, D. W.; Alheim, R. J.; Leavitt, J. J. *J. Am. Chem. Soc.* **1957**, *79*, 427−429.
(20) Bloomfield, J. J. *J. Org. Chem.* **1961**, *26*, 4112−4115.

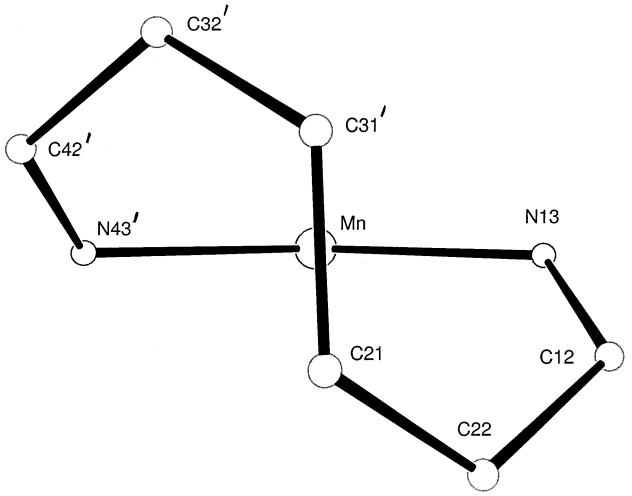


**Figure 3.** Nine-membered ring in one of the enantiomeric cations in *rac*-**6**.

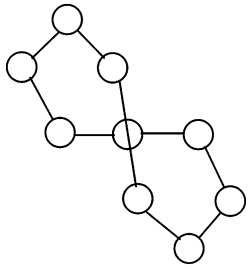

**Figure 4.** Twist−boat−boat conformation of a puckered nine-membered ring.

distances between *nearly-eclipsed*, slightly diverging imidazole fragments indicative of strong $\pi-\pi$ interactions.[21]

In *rac*-**5**·$(ClO_4)_2$ and *rac*-**6**·$(ClO_4)_2$, both cations and anions exhibit crystallographically imposed 2-fold symmetry with the metal ions and one perchlorate Cl atom located on 2a sites (0, 0, *z*) and the other Cl atom located on 2b sites (0, $^1/_2$, *z*). Perchlorate groups utilizing the 2b sites are ordered, while those on the 2a sites have one of the four oxygen atoms located on the 2-fold axis, and, as a consequence, three of the four oxygen atoms are disordered. The chelating benzimidazole ligands and metal ions form nine-membered rings whose conformation (Figure 3) is best described as twist−boat−boat (Figure 4), one of the 16 symmetrical conformations characteristic of nine-membered rings.[22] In the solid state, the chelate rings are effectively rigid and chiral. In a given cation, the ligands are related by crystallographic 2-fold axes and therefore must have the same handedness (*R*,*R* or *S*,*S*). Glide-plane operations convert one enantiomer to the other; hence, each unit cell contains an equal number of *R*,*R* and *S*,*S* cations, and crystals of **5**·$(ClO_4)_2$ and **6**·$(ClO_4)_2$ are racemic salts. Individual cations also contain approximate 2-fold axes normal to each other and the crystallographically imposed 2-fold axis, giving them effective 222 ($D_2$) site symmetry.

In summary, cations *rac*-**5** and *rac*-**6** exhibit $D_2$-distorted-tetrahedral coordination geometries, with comparable N−M−N bond angles, phenyl−phenyl dihedral angles, and phenyl−benzimidazole dihedral angles equal to within ±1°, indicating the extent to which the two cations are isostructural. A major difference between them is the M−N distances: the Mn−N lengths are on average 0.056 Å longer than the Fe−N distances, a difference attributable[23] primarily to the difference in ionic radii of the metals rather than the crystal-field effects, which are expected to be small for tetrahedral complexes. For tetrahedral complexes, 10 Dq is relatively small and, consequently, the crystal-field effects are expected to be small.

To our knowledge, *rac*-**5** provides the first example of a structurally characterized, four-coordinate Fe(II) complex containing an Fe−N(benzimidazole) bond, while cations *rac*-**5** and *rac*-**6** provide the first examples of four-coordinate Mn(II) and Fe(II) ions ligated exclusively by benzimidazoles. Relatively uniform ligation is expected to make these species especially attractive for spectroscopic studies.

In *rac*-**5**, the Fe−N(benzimidazole) distance [2.078(4) Å] lies within the range reported[24a] [2.063−2.095 Å] for the Fe(II)−N(*N*-methylimidazole) linkages in two four-coordinate bis(*N*-methylimidazole) species but is significantly longer than the Fe(II)−N(N1-substituted benzimidazole) linkages (1.927−1.978 Å) reported[24b−d] for several six-coordinate species. The Cambridge Crystallographic Database gave no entries for four-coordinate species containing Mn−N(imidazole) bonds and only one entry, **8**,[11a] for a four-coordinate species with Mn−N(benzimidazole) bonds. The Mn−N distances in the dication *rac*-**6** [2.130(4), 2.138(4) Å] compare well with those in the neutral, nearly tetrahedral **8** [2.136(6), 2.170(5) Å] and with the Mn(II)−N(*N*-methylbenzimidazole) distances [2.118(2), 2.127(2) Å] in a five-coordinate complex with $MnN(benzimidazole)_2N(imine)_2Cl$ coordination.[25]

In contrast to the Mn−N distances, the intraligand N−Mn−N angle [96.8(2)°] in **8**, which contains a seven-membered chelate ring, is some 23° smaller than that [119.95(15)°, Table 2] associated with the nine-membered ring in *rac*-**6**. Both of the values are about 10−12° removed from the tetrahedral value but in opposite directions. In **8** and other first-row transition-metal $MLX_2$ (X = halogen) complexes with similar ligands,[11a] nearly tetrahedral coordination was attributed to restricted puckering associated with the presence of two double bonds in the seven-membered rings. In *rac*-**5** and *rac*-**6**, the nine-membered rings contain four aromatic bonds, one from each of the four planar groups in the ligand, and a similar effect may be operative.

**3. Electrochemical Studies.** The reference compound Zn(**4**)$_2$·$(ClO_4)_2$ displayed no oxidations or reductions over

(21) Stibrany, R. T.; Schugar, H. J.; Potenza, J. A. *Acta Crystallogr.* **2003**, *E59*, o693−o695.
(22) Evans, D. G.; Boeyens, J. C. A. *Acta Crystallogr.* **1990**, *B46*, 524−532.
(23) Chen, H.-J.; Zhang, L.-Z.; Cai, Z.-G.; Yang, G.; Chen, X.-M. *J. Chem. Soc., Dalton Trans.* **2000**, 2463−2466.
(24) (a) Forde, C. E.; Lough, A. J.; Morris, R. H.; Ramachandran, R. *Inorg. Chem.* **1996**, *35*, 2747−2751. (b) Charbonnière, L. J.; Williams, A. F.; Piguet, C.; Bernardinelli, G.; Rivara-Minten, E. *Chem.−Eur. J.* **1998**, *4*, 485−493. (c) Piguet, C.; Rivara-Minten, E.; Bernardinelli, G.; Bünzli, J.-C. G.; Hopfgartner, G. *J. Chem. Soc., Dalton Trans.* **1997**, 421−433. Piguet, C.; Bernardinelli, G.; Williams, A. F.; Bocquet, B. *Angew. Chem., Int. Ed. Engl.* **1995**, *34*, 582−584.
(25) Kwok, W. H.; Zhang, H.; Payra, P.; Duan, M.; Hung, S.-c.; Johnston, D. H.; Gallucci, J.; Skrzypczak-Jankun, E.; Chan, M. K. *Inorg. Chem.* **2000**, *39*, 2367−2376.

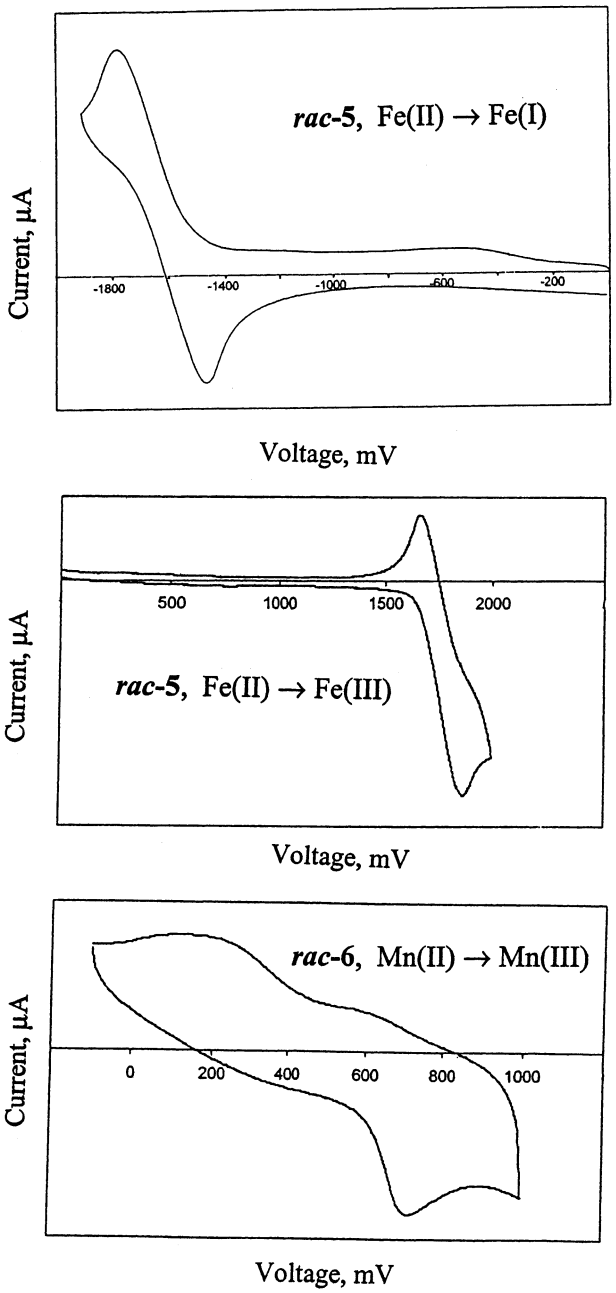


**Figure 5.** Cyclic voltammograms of (a) *rac*-**5** showing an Fe(II) → Fe(I) reduction, (b) *rac*-**5** showing an Fe(II) → Fe(III) oxidation, and (c) *rac*-**6** showing a quasi-reversible Mn(II) → Mn(III) oxidation. Measurements were made at room temperature in dichloromethane solutions containing 0.05 M tetra-*n*-butylammonium hexafluorophosphate. Complex concentrations ranged from 0.1 to 0.2 mM. Scan rate for a and b is 300 mV/s and that for c 50 mV/s.

the potential range studied for *rac*-**5** and *rac*-**6**. *rac*-**5** shows a one-electron reduction at $E_{1/2} = -1.60$ V (Figure 5a) corresponding to Fe(II) → Fe(I), as well as a one-electron oxidation at $E_{1/2} = 1.76$ V (Figure 5b) corresponding to Fe(II) → Fe(III). These potentials varied little for scan rates ranging from 25 to 300 mV/s for the oxidation (1.74−1.76 V) and from 50 to 300 mV/s for the reduction (−1.596 to −1.599 V). Over the same scan ranges, the difference between cathodic and anodic peak potentials decreased with the decreasing scan rate (from 238 to 108 mV for the Fe(II) oxidation and from 135 to 115 mV for the Fe(II) reduction)

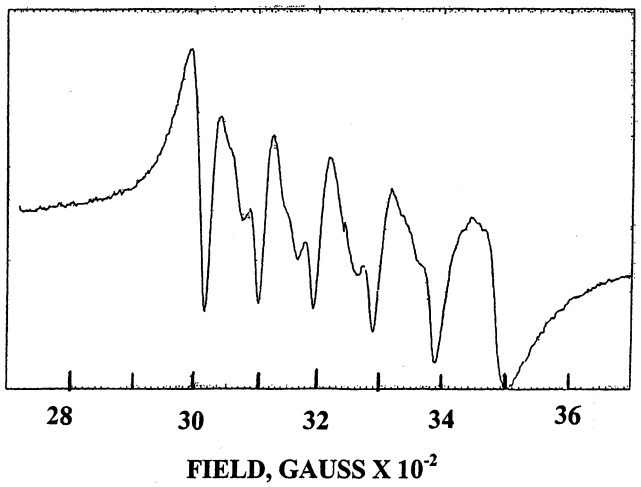


**Figure 6.** X-band EPR spectrum at 90 K of polycrystalline, nominally 3% Mn(II)-doped $Zn^{II}(\mathbf{4})_2 \cdot (ClO_4)_2$.

toward the value expected[26] (59 mV) for reversible one-electron processes. The electrochemical stability of the Fe(III) oxidation state in this system suggests that it might be possible to isolate an $Fe^{III}(\mathbf{4})_2$ complex, and we are currently attempting to do so. We are unaware of any structurally characterized tetrahedral $Fe^{III}N_4$ complexes. *rac*-**6** shows a broad, quasi-reversible one-electron oxidation at $E_{1/2} = 0.64$ V (Figure 5c) corresponding to Mn(II) → Mn(III), as well as an irreversible oxidation at $E_{1/2} = 1.36$ V corresponding to Mn(III) → Mn(IV).

**4. Magnetic Studies.** At room temperature, dichloromethane solutions of *rac*-$\mathbf{6} \cdot (ClO_4)_2$ exhibited broad X-band EPR spectra centered at $g \sim 2.0$ with few distinguishing features; these spectra did not noticeably sharpen at 77 K. The poorly resolved Mn(II) hyperfine coupling constant was estimated to be ∼100 G ($90 \times 10^{-4}$ cm$^{-1}$). Improved resolution (Figure 6) was obtained when the isostructural Zn(II) analogue[12] of *rac*-$\mathbf{6} \cdot (ClO_4)_2$ was doped at a nominal 3% level with Mn(II). The spectrum exhibits the characteristic six-line Mn(II) hyperfine coupling along with additional structure whose origin is uncertain. Recent studies have shown that axial and rhombic zero-field-splitting (ZFS) effects, which can contribute to the hyperfine structure exhibited by Mn(II) chromophores, are difficult to simulate convincingly for X band spectra;[27a] however, studies at considerably higher frequencies have allowed axial and rhombic ZFS effects to be quantified for a distorted-tetrahedral Mn(II) complex.[27b] The observed $g$ value [2.003(1)] is typical for a sextet ground-state Mn(II) ion (see the magnetic susceptibility results), which cannot spin−orbit couple to the excited ligand-field (LF) states, all of which

(26) Skoog, D. A.; Holler, F. J.; Nieman, T. A. *Principles of Instrumental Analysis*, 5th ed.; Harcourt Brace: Philadelphia, PA, 1998; Chapter 25, pp 639−672.

(27) (a) Coffino, A. R.; Peisach, J. *J. Magn. Reson., Ser. B* **1996**, *111*, 127−134. (b) Wood, R. M.; Stucker, D. M.; Jones, L. M.; Lynch, W. B.; Misra, S. K.; Freed, J. H. *Inorg. Chem.* **1999**, *38*, 5384−5388. (c) Manson, J. L.; Buschmann, W. E.; Miller, J. S. *Inorg. Chem.* **2001**, *40*, 1926−1935. (d) Chan, S. I.; Fung, B. M.; Lütje, H. *J. Chem. Phys.* **1967**, *47*, 2121−2130. (e) Tsay, F.-D.; Helmholz, L. *J. Chem. Phys.* **1969**, *50*, 2642−2650. (f) Olender, Z.; Goldfarb, D.; Batista, J. *J. Am. Chem. Soc.* **1993**, *115*, 1106−1114.

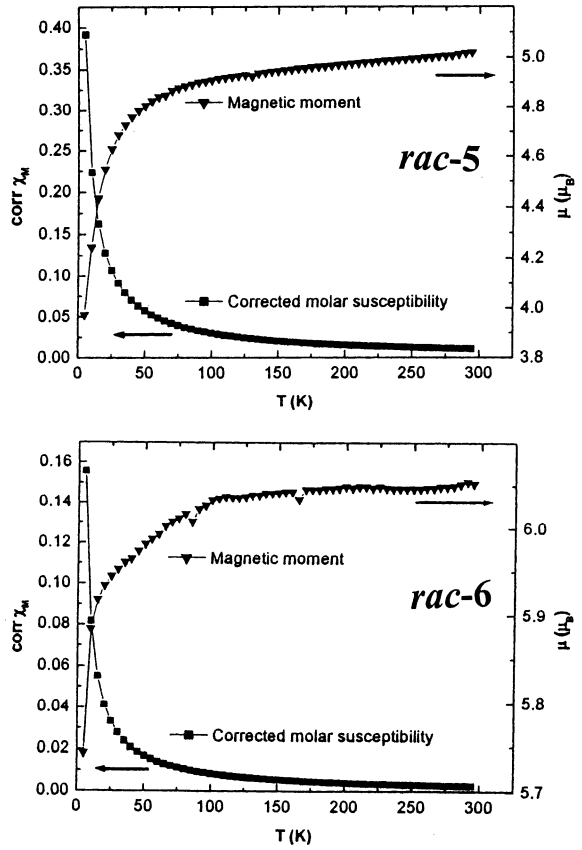


**Figure 7.** Magnetic susceptibilities in emu/mol and magnetic moments of (a) *rac*-**5**·$(ClO_4)_2$ and (b) *rac*-**6**·$(ClO_4)_2$ over the 5−295 K temperature range.

carry lower spin multiplicities. Moreover, in *rac*-**6**·$(ClO_4)_2$, Mn(II) is bound to N-donor atoms that cannot introduce substantial ligand-supplied spin−orbit effects. Smaller Mn coupling (65−79 G) has been reported for several tetrahedral Mn(II) complexes, whereas larger coupling (86−93 G) appears to be characteristic of octahedral Mn(II) chromophores.[27c−f] The trend of increased Mn hyperfine coupling reported for octahedral Mn(II) complexes relative to their regular tetrahedral analogues might not extend to the case of low-symmetry, nearly tetrahedral Mn(II) chromophores such as *rac*-**6**, which exhibits $C_2$ crystallographic and approximate $D_2$ site symmetry.

Dichloromethane solutions of *rac*-**5**·$(ClO_4)_2$ were EPR-silent at the X band at both room temperature and 77 K. As is typical for high-spin Fe(II) complexes, ZFS (see below) for *rac*-**5**·$(ClO_4)_2$ exceeds the available microwave energy of about 0.3 $cm^{-1}$ at the X-band (ca. 9 GHz) frequencies. Higher frequency EPR spectrometers (>94 GHz) are required to obtain energies large enough to pump the $\Delta m_s = 1$ transitions of non-Kramers $S = 2$ Fe(II) complexes showing ZFS.[28]

Corrected magnetic susceptibilities and magnetic moments of *rac*-**5**·$(ClO_4)_2$ and *rac*-**6**·$(ClO_4)_2$ from 5 to 295 K are shown in Figure 7. The magnetic moment of *rac*-**6**·$(ClO_4)_2$ is close to the spin-only value (5.92 $\mu_B$) for an $S = {}^5/_2$ Mn(II) system. As noted above, spin−orbit contributions are not expected for the $^6A_1$ ground state, consonant with the modest decrease in the magnetic moment from 6.05 $\mu_B$ at 295 K to 5.92 $\mu_B$ at 15 K. The magnetic moment of *rac*-**5**·$(ClO_4)_2$ at 295 K is increased slightly from the spin-only moment (4.90 $\mu_B$) to 5.02 $\mu_B$ possibly owing to an orbital contribution, which is allowed for this approximately tetrahedral high-spin $d^6$ Fe(II) complex.[29a] Upon cooling to 50 K, a slow decrease to 4.81 $\mu_B$ is observed, followed by a more pronounced falloff to 3.97 $\mu_B$ as the temperature is decreased to 5 K. The latter behavior is characteristic of Fe(II) complexes exhibiting positive ZFS.[30−32]

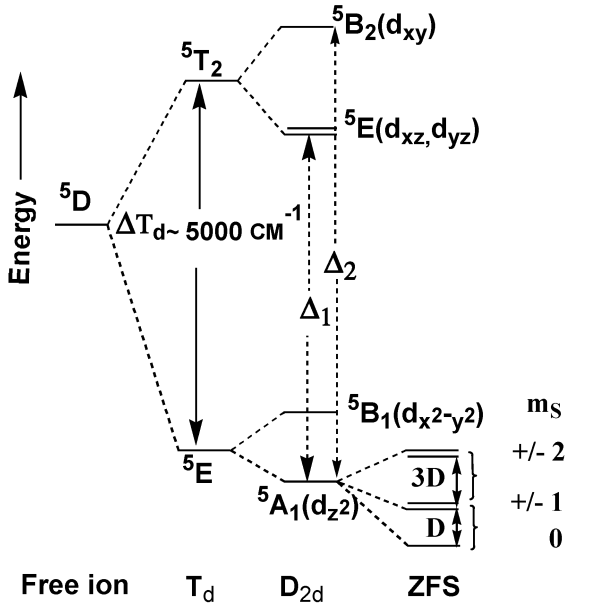


**Figure 8.** Energy level diagram for a $D_{2d}$-flattened pseudotetrahedral Fe(II) complex.

As noted above, the *R*,*R* and *S*,*S* Fe(II) chromophores in *rac*-**5**·$(ClO_4)_2$ adopt flattened, nearly tetrahedral geometries with apparent $D_2$ symmetry (three perpendicular 2-fold axes), even though only one 2-fold axis is crystallographically required. This latter axis is positioned perpendicular to the direction of flattening, a structural feature previously noted for the Ni(II) and Co(II) complexes of a related bidentate bis(imidazole)biphenyl ligand.[9] Although the chirality of individual cations precludes point symmetry containing mirror planes or centers of symmetry, the spectroscopically effective site symmetry of the bare $Fe^{II}N_4$ subunits in *rac*-**5** could be as high as $D_{2d}$. The energy level diagram for a $D_{2d}$-flattened pseudotetrahedral Fe(II) complex (Figure 8) shows the split LF transitions $\Delta_1$ and $\Delta_2$ (see the Electronic-Spectral Studies section below) and a positive ZFS parameter *D* arising from spin−orbit coupling of the $^5A_1$ ($d_{z^2}$) ground state.

(28) Knapp, M. J.; Krzystek, J.; Brunel, L.-C.; Hendrickson, D. N. *Inorg. Chem.* **2000**, *39*, 281−288.

(29) (a) Mabbs, F. E.; Machin, D. J. *Magnetism and Transition Metal Complexes*; Chapman and Hall: London, England, 1973; pp 20 and 21. (b) Mabbs, F. E.; Machin, D. J. *Magnetism and Transition Metal Complexes*; Chapman and Hall: London, England, 1973; pp 15 and 16.

(30) Edwards, P. R.; Johnson, C. E.; Williams, R. J. P. *J. Chem. Phys.* **1967**, *47*, 2074−2082.

(31) Dockum, B. W.; Reiff, W. M. *Inorg. Chim. Acta* **1986**, *120*, 61−76.

(32) Solomon, E. I.; Pavel, E. G.; Loeb, K. E.; Campochiaro, C. *Coord. Chem. Rev.* **1995**, *144*, 369−460.

*D* values for four pseudotetrahedral Fe(II) complexes have been measured by combined Mossbauer/magnetic susceptibility studies and that of a fifth complex by independent Mossbauer, far-infrared absorption, and high-frequency EPR spectroscopies. The reported *D* values span the range of $-5$ to $+11.6$ cm$^{-1}$. An estimate of *D* for *rac*-**5**·$(ClO_4)_2$ may be obtained from the LF theory using the relationship $D = 3\lambda^2/\Delta_1$, where $\lambda$ is the spin−orbit coupling constant and $\Delta_1$ is the energy separation between the $^5$E excited state and the $^5A_1$ ($d_{z^2}$) ground state (Figure 8).[32] The free-ion value of $\lambda$ for Fe(II) is 107 cm$^{-1}$ and is thought to be reduced by covalency in Fe(II) complexes to ∼80 cm$^{-1}$.[28,30,32] If $\Delta_1$ is taken to be 5000 cm$^{-1}$, the average of the two lowest LF absorptions (see Electronic-Spectral Studies section below), the estimated value of *D* is ∼4 cm$^{-1}$.

Although none of the *D* values reported in the literature is based solely upon magnetic susceptibility data, we attempted to estimate *D*, ZFS, and *g* values from a detailed analysis of low temperature susceptibility data for *rac*-**5**·$(ClO_4)_2$. A fresh sample was prepared, recrystallized twice, ground to a fine powder, and pressed into a pellet to minimize any preferential orientation of the crystallites in the magnetic field. Susceptibility data were recorded at ∼0.25 K intervals over the 2−50 K temperature range, and attempts were made, using nonlinear least-squares methods, to fit the data to the following expression for the molar susceptibility, $\chi_M$, which was derived for the $D_{2d}$ symmetry case:[30,33]

$$\chi_M = \frac{1}{3}\chi_{\parallel} + \frac{2}{3}\chi_{\perp} = \left(\frac{2N\beta^2 g_{\parallel}^2}{3kT}\right)\left(\frac{e^{-d} + 4e^{-4d}}{1 + 2e^{-d} + 2e^{-4d}}\right) + \left(\frac{4N\beta^2 g_{\perp}^2}{9D}\right)\left(\frac{9 - 7e^{-d} - 2e^{-4d}}{1 + 2e^{-d} + 2e^{-4d}}\right)$$

where $d = D/kT$ and $N\beta^2/3k = 0.1251$.

The results, presented graphically in the Supporting Information, are summarized as follows. The nonlinear least-squares fit is initial-conditions dependent, and, for example, similar, stable, and reproducible fits could be obtained, yielding positive or negative *D* values, starting from different positive or negative *D* values, respectively. The values obtained for the two minima are as follows: $D = 2.1(5)$ cm$^{-1}$, $g_{\parallel} = 2.41(9)$, and $g_{\perp} = 1.54(8)$; $D = -6.82(4)$ cm$^{-1}$, $g_{\parallel} = 1.769(1)$, and $g_{\perp} = 2.063(2)$. The second set of values corresponds to the "best" fit, i.e., the one with the lowest $\chi^2$ value. With $g_{\parallel}$ and $g_{\perp}$ each fixed at 2.0, the resulting *D* value is $-28 \pm 3$ cm$^{-1}$, and the fit is substantially inferior. When *g* and *D* are allowed to vary independently, *g* values significantly less than 2.0 are obtained, a physically impossible result for a $d^6$ Fe(II) ion with a greater than half-filled d subshell. These difficulties suggest that the equation above is unsuitable for rhombically split sites because, among other things, $\chi_M$ no longer is equal to $^1/_3\chi_{\parallel} + {}^2/_3\chi_{\perp}$. As a result, neither an unambiguous value of *D* nor reasonable *g* values could be extracted from an analysis of the low-temperature magnetic susceptibility data. For a distorted-tetrahedral $Fe(SPh)_4^{2-}$ chromophore, the rhombic contribution to ZFS was calculated to be $+1.4$ cm$^{-1}$, a substantial fraction of the axial contribution, $+5.8$ cm$^{-1}$.[28]

Finally, the susceptibility data closely follow Curie−Weiss behavior with $C = 3.00$ and $\theta = -3.3$ K. The relationship $g_{eff} = 2.828[C/(S(S+1))]^{1/2}$ with $S = 2$ gives a plausible *g* value of 2.00. However, the substantial size of ligand **4** suggests that that *rac*-**5**·$(ClO_4)_2$ is magnetically dilute and, therefore, that a finite value of $\theta$ does not need to signify a magnetic interaction between the complexes. It merely means that a Curie−Weiss analysis of a magnetically noninteracting complex can effectively mask whatever phenomena actually are contributing to the observed magnetic behavior. For Fe(II), the well-documented ZFS may be obscured.[29b]

**Table 3.** Summary of Deconvoluted Electronic and Reflectance Spectra

| substance | energy (cm$^{-1}$) | $\epsilon^a$ |
|---|---|---|
| **4** | 33 100 | 20 000 |
| | 40 700 | 54 000 |
| | 48 100 | 150 000 |
| *rac*-**5**·$(ClO_4)_2$ | 4700[b] | broad |
| | 5300[b] | broad |
| | ∼6000[b] | shoulder |
| | 35 900 | 88 000 |
| | 43 200 | 11 000 |
| | ∼50 000 | 370 000 |
| *rac*-**6**·$(ClO_4)_2$ | 35 200 | 19 000 |
| | 42 600 | 31 000 |
| | ∼50 000 | 110 000 |

[a] Extinction coefficients are normalized to one ligand **4**. [b] Reflectance data.

**5. Electronic-Spectral Studies.** Electronic spectra of **4**, *rac*-**5**·$(ClO_4)_2$, and *rac*-**6**·$(ClO_4)_2$ are shown in Figure 9 and summarized in Table 3. The deconvoluted spectrum of **4** shows three broad overlapping absorptions centered at 33 000 ($\epsilon = 20\,000$), 40 700 ($\epsilon = 54\,000$), and 48 100 ($\epsilon = 150\,000$) cm$^{-1}$. The positions and intensities of these bands correspond roughly to the composite absorptions of its biphenyl and benzimidazole subunits. Biphenyl[34a] shows a broad absorption at 40 500 cm$^{-1}$ ($\epsilon = 19\,300$), whereas benzimidazole and 2-alkyl-substituted benzimidazoles show progressions of absorptions[34b] centered at ∼35 600 cm$^{-1}$ ($\epsilon \sim 6000$) and ∼40 000 cm$^{-1}$ ($\epsilon \sim 6000$), along with a more intense absorption at 47 600 cm$^{-1}$ ($\epsilon \sim 27\,900$). These benzimidazole extinction coefficients should be doubled to place them and the spectrum of **4**, which contains two benzimidazole units, on the same scale. A recent study of benzimidazole[35] suggests that the band system at ∼35 600 cm$^{-1}$ has mixed but predominantly HOMO → LUMO + 1 orbital character. The flanking higher-energy pattern at ∼40 000 cm$^{-1}$ is thought to contain a HOMO → LUMO character, whereas the highest-energy absorption was assigned as predominantly HOMO − 1 → LUMO + 1. Ultraviolet spectra of *rac*-**5**·$(ClO_4)_2$ and *rac*-**6**·$(ClO_4)_2$ are dominated by the absorptions of ligand **4** blue-shifted by ∼2000−3000 cm$^{-1}$. Possible

(33) O'Connor, C. J. In *Progress in Inorganic Chemistry*; Lippard, S. J., Ed.; Wiley: New York, 1982; pp 232 and 233.

(34) (a) In *Stadler Handbook of Ultraviolet Spectra*; Simons, W. W., Ed.; Stadler Research Laboratories: Philadelphia, PA, 1979; p 21, spectrum 171. (b) In *Stadler Handbook of Ultraviolet Spectra*; Simons, W. W., Ed.; Stadler Research Laboratories: Philadelphia, PA, 1979; pp 182 and 183, spectra 738 and 739.

(35) Borin, A. C.; Serrano-Andrés, L. *Chem. Phys.* **2000**, *262*, 253−265.

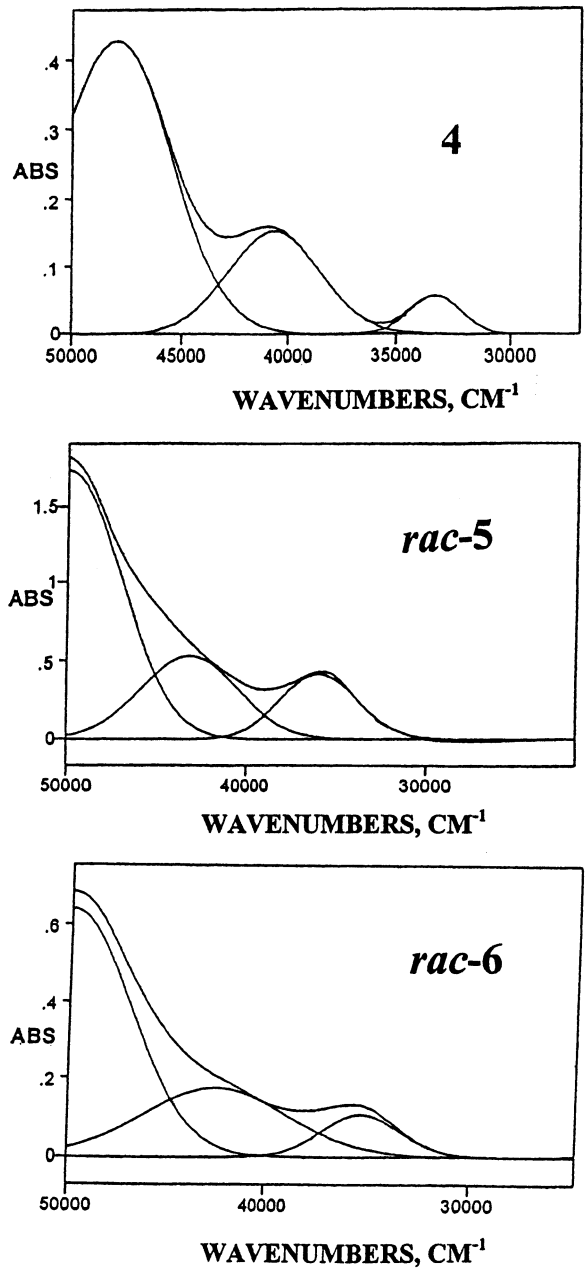


**Figure 9.** Ultraviolet spectra (ABS = absorbance) in an acetonitrile solution at room temperature of (a) **4** (14.1 $\mu$M, 2 mm path), (b) *rac*-**5**·$(ClO_4)_2$ (23.4 $\mu$M, 1 mm path), and (c) *rac*-**6**·$(ClO_4)_2$ (28.6 $\mu$M, 1 mm path).

charge-transfer and/or LF absorptions in the UV region are obscured by the more intense ligand absorptions.

In both the solution and reflectance spectra of high-spin *rac*-**6**·$(ClO_4)_2$, the expected spin-forbidden sextet → quartet LF absorptions were too weak to characterize clearly. Measurements of such absorptions typically require low temperature single-crystal studies.[36] In contrast, the more intense low-energy LF absorptions expected for high-spin *rac*-**5**·$(ClO_4)_2$ were readily seen in the room-temperature reflectance spectra. The reflectance spectrum of *rac*-**6**·$(ClO_4)_2$ was used as a control to identify the absorptions in this region due to ligand infrared vibrational overtones. LF absorptions of tetrahedral Mn(II) are not observed at energies below 18 000 $cm^{-1}$.[36−38] Broad absorptions of *rac*-**5**·$(ClO_4)_2$ at 4700 and 5300 $cm^{-1}$ are attributed to $^5A_1 \rightarrow {}^5E$ absorptions ($\Delta_1$ in Figure 8) of this approximately $D_{2d}$ Fe(II) chromophore split by the reduction of symmetry to $D_2$ as noted in the crystallographic discussion. The broad shoulder at ~6000 $cm^{-1}$ is assigned to the expected $^5A_1 \rightarrow {}^5B_2$ transition shown as $\Delta_2$ in Figure 8.[38′]

## Conclusions

**4**, with four planar groups and three connecting "hinges", acts as a geometrically constraining bidentate ligand. With Fe(II) and Mn(II), high-spin nearly tetrahedral complexes containing $M^{II}(\mathbf{4})_2$ cations are formed. Ligation yields rigid, chiral nine-membered M(**4**) rings, resulting in cations with *R,R* or *S,S* stereochemistry. Crystals of $Fe^{II}(\mathbf{4})_2$·$(ClO_4)_2$ and $Mn^{II}(\mathbf{4})_2$·$(ClO_4)_2$ are isomorphous racemates with equal numbers of *R,R* and *S,S* cations in each unit cell. $Mn^{II}(\mathbf{4})_2$·$(ClO_4)_2$ exhibits a Mn(II) → Mn(III) oxidation at $E_{1/2} = 0.64$ V. The corresponding Fe(II) → Fe(III) oxidation at $E_{1/2} = 1.76$ V suggests the possibility of isolating an unusual pseudotetrahedral $Fe^{III}N(BzIm)_4$ species. Ultraviolet spectra of the Fe(II) and Mn(II) complexes are dominated by absorptions of ligand **4** blue-shifted by approximately 2000−3000 $cm^{-1}$. LF absorptions were observed for the Fe(II) chromophore; those expected for the Mn(II) analogue were too weak to be observed above the background of the tailing UV absorptions. Magnetic susceptibility studies show that $Mn^{II}(\mathbf{4})_2$·$(ClO_4)_2$ behaves as a simple, high-spin paramagnet, whereas the falloff in the magnetic moment shown by $Fe^{II}(\mathbf{4})_2$·$(ClO_4)_2$ from 5.02 $\mu_B$ at 295 K to 3.97 $\mu_B$ at 5 K is indicative of ZFS. From LF considerations, the ZFS parameter $D$ was estimated to be ~4 $cm^{-1}$.

**Acknowledgment.** Preliminary variable-temperature magnetic susceptibility studies were performed by Guerman Popov in the laboratory of Professor Martha Greenblatt. We thank Dr. Popov for his assistance.

**Supporting Information Available:** Tables in CIF format containing (1) additional details regarding the solution of the structures, (2) information on data collection and refinement of the structures, (3) atomic coordinates, (4) anisotropic thermal parameters, (5) bond lengths, and (6) bond and torsional angles for **4**, *rac*-**5**·$(ClO_4)_2$, and *rac*-**6**·$(ClO_4)_2$. The molar susceptibility of *rac*-**5**·$(2ClO_4)_2$ over the 2−50 K temperature range and fitting results for the molar susceptibility using the equation in the text. This material is available free of charge via the Internet at http://pubs.acs.org.

IC030180O

(36) Siiman, O.; Gray, H. B. *Inorg. Chem.* **1974**, *13*, 1185−1191 and references therein.

(37) Lever, A. P. B. *Inorganic Electronic Spectroscopy*, 2nd ed.; Elsevier: New York, 1984; p 450.

(38) Forster, D.; Goodgame, D. M. L. *Inorg. Chem.* **1965**, *4*, 1712−1716.